

# Comparing the Performance of Co-Axial and Parallel-Plate Gas-Fed PPTs \*

J.K. Ziemer<sup>†</sup> and E.Y. Choueiri<sup>‡</sup>  
MAE Dept., Princeton University, Princeton, New Jersey 08544

D. Birx  
Science Research Laboratory Inc., Sommerville, MA 02143

IEPC-99-209<sup>§</sup>

## Abstract

We present the measured performance of four different gas-fed pulsed plasma thrusters (GFPPTs) over a wide range of operating conditions using argon and water vapor propellant with both co-axial and parallel-plate electrode configurations. It is shown that the inductance-per-unit-length has an influence on performance, however, not always to the extent that is predicted by an electromagnetic model for acceleration in GFPPT discharges. In these cases, the discrepancies are suspected to be related to larger wall losses. Although the highest value of inductance-per-unit-length tested using parallel-plate electrodes is twice that of one of the co-axial electrode geometries, the co-axial GFPPT is shown to have a higher measured performance.

## 1 Introduction

Since their invention, the geometry of pulsed plasma thruster (PPT) electrodes has been modified extensively in attempts to improve their performance. Due to the complex multi-variable nature of PPT design, investigators have turned to empirical, parametric studies to show how electrode configuration impact performance. Specifically, the advantages and disadvantages of the two main types of electrode geometry, co-axial and parallel-plate, have always been a topic of debate. Experimental data has yet to uncover the best configuration over a wide range of operational parameters.

Recent activity at the Electric Propulsion and Plasma Dynamics Lab (EPPDyL) at Princeton in cooperation with Science Research Laboratory, Inc. (SRL) and the Advanced Propulsion Group at NASA Jet Propulsion Laboratory (JPL) has focused on designing gas-fed PPTs (GFPPTs) with modular components such as capacitance[1] and electrode geometry[2] to measure the various effects on performance. Through analytic models of electromagnetic acceleration, the performance of GFPPTs is expected to scale with the square-root of the product of capacitance and inductance-per-unit-length and not depend on propellant mass. In actual thrusters where proper mass loading is an important concern, however, the mass utilization efficiency is shown to scale with the inverse of capacitance. This leaves the inductance-per-unit-length as the most likely design parameter that can influence overall performance over a wide range of operational conditions.

The purpose of this paper is twofold: one, to help verify the relation of inductance-per-unit-length (and hence electrode geometry) to GFPPT performance in a systematic way, and, two, to discuss which electrode geometry (co-axial or parallel-plate) is better for overall performance. The paper begins by describing the four different GFPPTs used in performance testing. The following section defines the propellant utilization efficiency and derives a theoretical prediction for the effect of inductance-per-unit-length on performance. Next, performance measurements are presented and trends in the data are used to discuss changes in performance due to inductance-per-unit-length. Finally, there is a discussion of other factors that are yet to be quantified which could influence future debates on which electrode geometry is truly the best.

---

\*Research supported by the Air Force Office of Scientific Research, grant number: F49620-95-1-0291, NASA JPL's Advanced Propulsion Group, and the Plasma Science and Technology Program at the Princeton Plasma Physics Lab.

<sup>†</sup>Graduate Student, Research Assistant. Member AIAA.

<sup>‡</sup>Chief Scientist at EPPDyL. Assistant Professor, Applied Physics Group. Senior Member AIAA.

<sup>§</sup>Presented at the 26<sup>th</sup> International Electric Propulsion Conference, Kitakyushu, JAPAN, October 17-21, 1999.

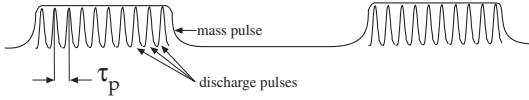


Figure 1: Schematic drawing of the high-repetition pulse train in SRL-GFPPTs.

## 2 The SRL Family of GFPPTs

The SRL Family of GFPPTs has been described before in refs. [1, 2] and will only be summarized here. SRL-GFPPTs use modern pulse forming technology to create a series of high-repetition rate pulses. During a burst of pulses, propellant flows at a constant rate just filling the discharge volume before the next pulse occurs. This is shown schematically in Fig. 1. The performance of these GFPPTs is related to the driving capacitance, electrode configuration, propellant loading, and many other parameters that have been explored through the creation of many generations of GFPPT designs. All of the designs tested in this study are illustrated in a table at the end of this paper (Fig. 8) that includes information on all relevant performance parameters. Of these thrusters, only PT8 and PT9 have not been introduced in the literature and a more detailed description of them follows.

### 2.1 PT8

PT8 belongs to the group of GFPPTs including PT6 and PT7 called the quad thrusters. Compared to the first quads, PT8 uses a new lower-energy RF system to initiate the discharge, a set of ferrite blocks around the electrodes to reduced magnetic field fringing effects, and a new propellant injection scheme to reduce the cold gas velocity and improve propellant utilization.

### 2.2 PT9

PT9 uses the capacitors and thruster body from PT5 with a modular set of parallel-plate electrodes for testing various values of inductance-per-unit-length. All the electrodes are made from 1/8" thick 70% tungsten 30% copper plates of 1" x 4" (width x length) or 1/2" x 4" dimensions. There are two places to mount the electrodes at distances of either 1" or 1/2" apart. This gives four different electrode configurations and three different inductance-per-unit-length values. PT9 uses a high voltage (2 kV) low energy (50 mJ) trigger discharge between a sharp, 10 mil tungsten wire and the cathode of the thruster in an attempt to reduce erosion rates. Although erosion rates have yet to be measured accurately for

this thruster, visible damage to thruster components is greatly reduced compared to damage seen in life-tests with PT7 [2] over the same number of discharge pulses. The main purpose of PT9 is to test different inductance-per-unit-length configurations at similar operational conditions to those tested with the co-axial set of electrodes in PT5.

## 3 Performance Considerations for Both Geometries

This section of the paper will document the calculations used to compare the performance of *both* co-axial and parallel-plate GFPPTs tested at EP-PDyL and NASA JPL. Conventional definitions for efficiency, thrust-to-power ratio, and specific impulse will be used as defined in ref. [1]. A derivation of the propellant mass utilization efficiency is shown to depend on electrode length, discharge pulse frequency and propellant type. The derivation of this efficiency helps to show why the capacitance can not be raised to an arbitrary value without possibly wasting propellant. Through the introduction of an electromagnetic acceleration model for GFPPT discharges, the trade-offs between predicted thruster performance and propellant utilization will be discussed and the inductance-per-unit-length is found to be an important parameter in performance scaling. Finally the quantitative differences in inductance-per-unit-length between the two geometries will be presented.

### 3.1 Propellant Utilization Efficiency

In high repetition rate GFPPTs the mass bit value used for overall performance calculations is a ratio of the the steady mass flow rate,  $\dot{m}$ , during a burst and the pulse frequency within a burst,  $1/\tau_p$ . Depending on the electrode length and the mean thermal velocity of the cold gas, some of the mass included in this efficiency calculation might not actually be accelerated by the discharge. Using the maximum possible thermal velocity,  $v_{th}$ , the spatial extent of the cold-gas column before each discharge can be estimated by,

$$\ell_{gas} = v_{th}\tau_p = \tau_p \sqrt{\frac{3kT}{m_w}}. \quad (1)$$

As an example, using argon and a pulse frequency of 4 kHz,  $\ell_{gas} \approx 10$  cm, and unless the electrodes are made to be at least 10 cm long, then some portion of the gas will be wasted.

The mass utilization efficiency,  $\eta_{pu}$ , can now be defined as the ratio of the electrode length,  $\ell_{elec}$ , to the gas column length,  $\ell_{gas}$ .

$$\eta_{pu} \equiv \frac{\ell_{elec}}{\ell_{gas}} = \frac{\ell_{elec}}{\tau_p} \sqrt{\frac{m}{3kT}}. \quad (2)$$

Obviously even if the electrodes are longer than the gas column, the propellant utilization efficiency can not exceed 100%. In general,  $\eta_{pu}$  should be maximized for optimal performance although a high pulse frequency or long electrodes can have an adverse effect on performance as described in the next section.

### 3.2 System Wide Trade-offs for Maximizing Propellant Utilization

From Eq. (2), maximizing the propellant utilization efficiency can include selecting a large molecular weight propellant, pulsing at a high frequency, using long electrodes, or a combination of these prescriptions. Changing these parameters, however, may have an adverse effect on performance and there are recognizable trade-offs in terms of predicted electromagnetic performance. Ref. [1] derives the theoretical performance for a GFPPT discharge as,

$$\eta \propto \frac{\bar{u}_e}{2} \sqrt{\frac{CL'}{\ell_{elec}}} \quad \frac{T}{P} \propto \sqrt{\frac{CL'}{\ell_{elec}}}, \quad (3)$$

where  $L'$  is introduced here as the inductance-per-unit-length. This relation assumes that the discharge is mainly an *inductive* load that reaches the end of the electrodes at the moment the capacitor is fully drained. It represents the *maximum* obtainable performance when the mass utilization efficiency is 100%. The following paragraphs describe the trade-offs in maximizing the propellant utilization efficiency.

**Large Molecular Weight Propellant.** Using a large molecular weight propellant to increase  $\eta_{pu}$  appears to be the best choice of parameters to change. At a fixed plenum temperature, larger molecular weight propellants yield a lower thermal velocity. Compared to smaller molecular weight propellants at similar mass loading conditions, heavier molecules will produce a smaller value of gas-dynamic pressure in the discharge chamber before the pulse begins. The conductivity of the plasma and possibly frozen flow losses, however, could adversely effect performance through the choice of propellant molecule although this has not yet been extensively studied in GFPPTs. Experimental measurements of performance (see Section 4.1) using PT8 with the same operational mass bit of argon or water vapor show that water vapor actually has a slightly higher efficiency although this trend is within the error of the experiment.

**High Pulse Frequency.** The minimum time between pulses (the fastest pulse frequency) is regulated by the time to charge the main capacitor. It is proportional to the capacitance magnitude and can be reduced by simply using smaller capacitance values

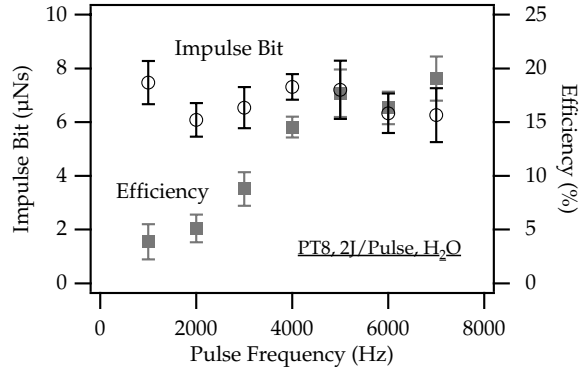


Figure 2: Impulse bit and efficiency as a function of pulse frequency for PT8 using water vapor for propellant at 2 J per pulse.

or increasing the charging current, however, the latter choice can also decrease the power conditioner performance. The benefit of setting the pulse rate to the maximum the capacitance will allow is shown in Fig. 2 where the efficiency increases to its maximum value as the pulse frequency increases. Notice that the impulse bit, and therefore the thrust-to-power ratio, does not change within the error of the measurement and is not directly dependent on the propellant utilization efficiency in GFPPTs. In addition, since the specific impulse calculation is also dependent on the propellant utilization efficiency, performance curves on graphs of efficiency vs. specific impulse will not change form, only relative magnitude.

A contrary argument to decreasing the capacitance can be seen from Eq. (3) and experimental evidence in ref. [1] which suggests that the performance of a GFPPT increases with the square-root of the capacitance. This trade-off between the discharge performance and the propellant utilization efficiency points to using smaller capacitances until  $\eta_{pu}$  is exactly unity. Yet, although the overall efficiency may now be optimized, the maximum *possible* performance (both efficiency and thrust-to-power) still occurs at the highest values of capacitance. Therefore, decreasing the capacitance of a GFPPT may not be the best way to improve the propellant utilization efficiency and should only be used if no other avenue is possible. At the same time, increasing the capacitance to boost performance makes it more and more difficult to obtain reasonable propellant utilization. This again points to using the inductance-per-unit-length parameter as a better way to increase performance as further described in Section 3.3.

**Electrode Length.** It can be seen from Eq. (3) that there is a complex trade-off between lengthen-

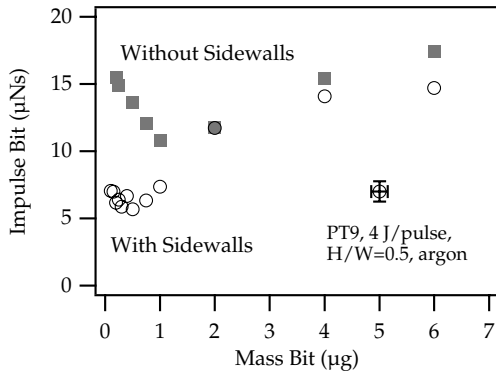


Figure 3: Effect of Pyrex side walls on performance as a function of mass bit for PT9 at 4J/pulse with 1'' x 1/2'' electrodes using argon.

ing the electrodes to use all the propellant effectively and a decrease in the predicted performance. At the same time, if the electrodes are short and the mass bit is small (typically where the highest performance occurs), then the current sheet will not reside within the electrodes long enough to absorb all the energy from the capacitor. In addition, the total inductance change with a short set of electrodes may not be large enough for efficient electromagnetic acceleration. Therefore, the electrode length and operational mass bit must be chosen so that  $\eta_{pu}$  is 100% and the current sheet reaches the end of the electrodes just as the capacitor is fully drained.

There is also the possible factor of increased viscous and heat transfer losses from longer electrodes. Previous estimates of viscous stress in quasi-steady MPD thrusters[3, 4] have shown through order-of-magnitude arguments that it is not a significant loss mechanism at high powers. In GFPPTs, this same analysis shows this to be true near the peak of the discharge when the current and voltage are large and the sheet velocity is relatively small. However, this is not true at later stages in the GFPPT discharge when the Lorentz force has decayed while the velocities are still high. With longer electrodes, viscous losses could significantly influence the final velocity.

In an attempt to quantify this experimentally, PT9 was tested using the same electrode geometry with and without Pyrex side walls. As shown in Fig. 3, the performance was *increased* when the Pyrex side walls were removed. It should be noted, however, that in the tests without the side-walls, the discharge was seen to periodically stretch out of the electrode volume during tests at low mass bits. At low mass bits, additional mass from erosion products and possibly spurious arc attachments can significantly impact the performance. Therefore, it was felt that all data used for comparison of PT9 with other con-

figurations should have Pyrex side walls to contain the discharge and minimize possible effects of erosion products. This effect was not seen at higher mass bits, however, and the effect of the side walls can still be noticed although it is a smaller increase.

### 3.3 Inductance-per-Unit-Length

The inductance-per-unit-length,  $L'$ , is one of the most important differences between parallel-plate and co-axial electrode geometries. As seen from Eq. (3), the performance of a GFPPT is predicted to scale with the square root of  $L'$ . Although previous experiments have already demonstrated that increasing the capacitance can improve performance, it may have an adverse effect on propellant utilization efficiency as shown in Section 3.2. This makes the possibility of increasing  $L'$  to improve performance even more important.

This quantity is calculated by integrating the magnetic flux through a volume enclosed by the discharge. The inductance gradient for a parallel-plate thruster can be estimated by treating the electrodes as a single-turn infinite coil with a uniform field,

$$L'_{pp} \approx \mu_0 \frac{H}{W}. \quad (4)$$

For a co-axial GFPPT, the calculation can be carried out directly and no approximation is necessary assuming a planar current sheet,

$$L'_{co-ax} = \frac{\mu_0}{2\pi} \ln \frac{r_{out}}{r_{in}}. \quad (5)$$

As other authors[5] have pointed out, however, most useful parallel-plate geometries have very non-uniform fields, and the fringing effects of finite-width electrodes must be taken into account. Using a conformal mapping technique to determine the electromagnetic fields in a parallel rail launcher, ref. [6] provides the necessary tabular data to determine the actual value of the inductance-per-unit-length for a given electrode aspect ratio. The graph in Fig. 4 shows the approximate  $L'$  value and the actual value  $L'$  for both parallel-plate and co-axial geometry which will be used for this study. The graph also provides a comparison of the  $L'$  values for all the GFPPTs tested here. The graph shows that the inductance-per-unit-length for a co-axial thruster and a parallel-plate thruster is similar if the co-axial thruster has a radius-ratio ten times the height-to-width ratio of a parallel plate thruster. In general, however, reasonable geometries for parallel-plate thrusters have a higher value of  $L'$  as is the case with most of the GFPPTs tested here.

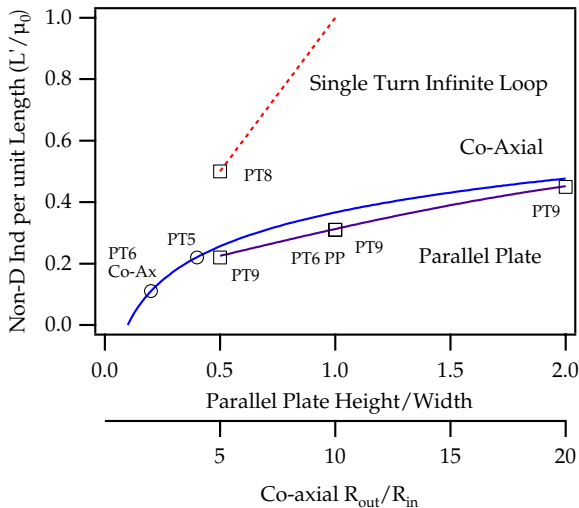


Figure 4: Normalized inductance gradient as a function of geometry for parallel-plate and co-axial electrodes.

## 4 Measured Performance of GFPPTs

Performance of four different GFPPTs have been measured over various mass bits, energy levels, capacitance values, etc. to form an extensive data base that can be used to compare the performance of co-axial vs. parallel-plate electrode geometries. Many of the experimental protocols and methods for calculating performance from the measured quantities have been documented previously [1, 2] and will not be repeated here. Performance measurements of the quad thrusters, PT6-PT8, were conducted at NASA JPL while PT5 and PT9 were tested at EPPDyL.

### 4.1 The Quad Series of SRL-GFPPT

The performance of PT6 and PT8 was measured with both parallel-plate and co-axial electrodes using argon and water vapor for propellant over many different mass bits. The discharge energy was kept constant at 2 J/pulse to form the performance database shown in Fig. 5. Note that at all directly comparable conditions, the performance of the parallel plate thrusters is better than that of the co-axial thruster.

**Inductance-per-Unit-Length Effects.** We believe that a majority of the trends in this quad-thruster database are due to changes in inductance-per-unit-length, however, this is not the only factor. For PT6, the open parallel-plate geometry had nearly double the performance of the co-axial electrodes. This could be both a result of the higher  $L'$  value

for the parallel-plate electrodes as well as the likely inefficient electromagnetic acceleration in the co-axial electrodes that experience such a small total inductance change.

In comparing the performance of the parallel-plate geometry of PT6 and the improved inductance-per-unit-length of PT8, there is not the expected 20% gain in performance except at the higher mass bit values. It is suspected that the confined nature of PT8's electrodes along with the extra side-walls provided by the ferrite blocks caused higher wall losses at the lowest mass bits and actually *decreased* performance. Still, the overall trends in the data suggest that there are potential benefits of the higher inductance-per-unit-length values associated with using parallel-plate geometry.

### 4.2 PT5 and PT9 Performance

The performance of PT5 has been fully documented in ref. [1] and only one set of conditions using 130  $\mu\text{F}$  at 4 J/pulse will be used here to compare co-axial vs. parallel plate electrodes. The parallel-plate thruster, PT9, was designed to test the impact of inductance-per-unit-length on performance in a controlled manner. Unfortunately, the trends in the measured data shown in Fig. 6 are not predicted by an electromagnetic model of acceleration. Other loss mechanisms may be playing a significant role in reducing the performance of the parallel plate thrusters. Figure 6 shows the performance of PT5 and PT9 over a variety of operational conditions and height-to-width ratios for PT9 electrodes. In all cases at comparable operating conditions, the co-axial electrodes outperform or at least match the performance of the parallel-plate configurations even with a factor of two increase in  $L'$ .

At low mass bits, all three parallel-plate electrode geometries have similar performance within the error of the measurements indicating that some other phenomena may be influencing the discharge propagation more significantly than electrode configuration. The best performance in terms of impulse bit and thrust-to-power ratio came from the 1" x 1" electrodes at high mass bit values which lends even further evidence that a more confined discharge volume could be reducing the performance beyond what increasing the inductance-per-unit-length provides.

## 5 Discussion

Although higher efficiency alone could be considered to be the strongest argument for choosing co-axial electrodes over parallel plate electrodes, there are other factors which should be considered. Among the most important of these, as yet, unquantified issues are possible current sheet acceleration profile losses.

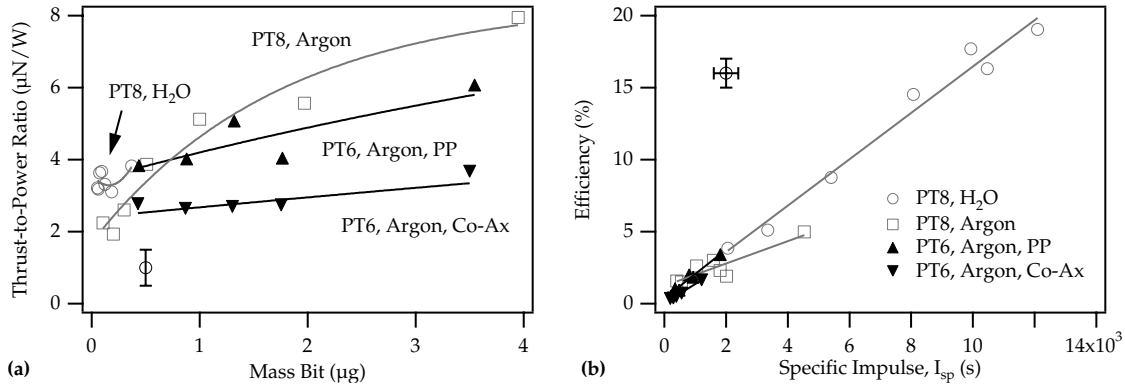


Figure 5: Efficiency and thrust-to-power ratio plotted against specific impulse and mass bit for PT6 with argon and PT8 with argon and water vapor. All data shown is taken at 2 J per pulse using a  $63 \mu\text{F}$  capacitor. A sample error bar for this data set is also shown.

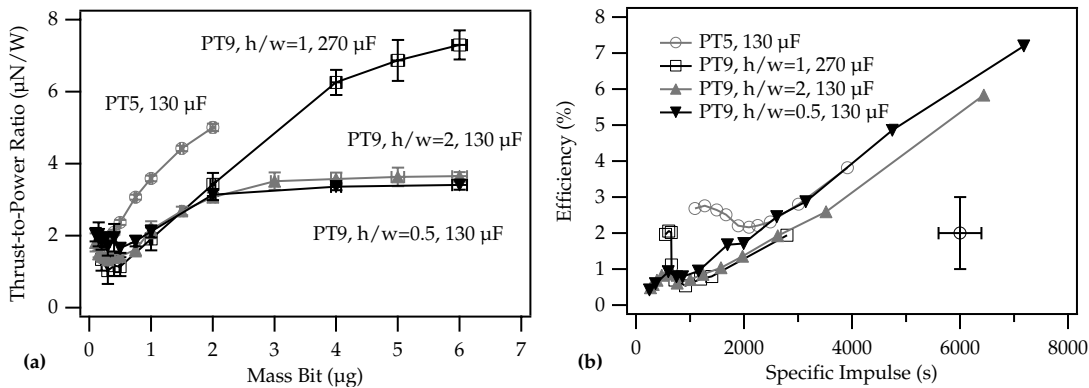


Figure 6: Efficiency and thrust-to-power ratio plotted against specific impulse and mass bit for PT5 and PT9 with varying height/width ratios. All data shown is taken at 4 J per pulse using either a 130 or 270  $\mu\text{F}$  capacitor bank. A sample error bar for this data set is also shown.

Current sheet profile losses can come in two different forms: a spatially non-uniform Lorentz Force acting on the current sheet, and an as yet unexplained canting seen in parallel plate thrusters that is currently under investigation at EPPDyL[7]. For co-axial thrusters, the current density and hence the magnetic field are both proportional to  $1/r$  giving a Lorentz force that increases rapidly at the center electrode as  $1/r^2$ . This non-uniformity would suggest that the current sheet runs along the center electrode very fast forming a cone-like structure which accelerates the gas in a non-axial manner. In more recent co-axial SRL-GFPPT designs an attempt is made to balance this non-uniform force by injecting more propellant near the center electrode.

The other type of profile loss has been discovered by viewing Imacon fast-framing camera pictures of

parallel-plate discharges on micro-second time scales. As shown in Fig. 7, the current sheet shows a bifurcation and canting with the leading edge always moving along the anode first. If this emission represents the current conduction location, then the acceleration will not be directed axially and performance losses will result. It is entirely possible that this same canting is occurring in co-axial thrusters. If this is true, then for the co-axial SRL-GFPPT designs where the center electrode is the anode, this could mean an even more elongated current sheet and higher profile losses. To measure this effect, future work at EPPDyL will include reversing the polarity of one of the co-axial thrusters to see if the two non-uniform profiles can counter-act each other. For parallel-plate thrusters, work is continuing at EPPDyL to understand and, if possible, eventually counteract this

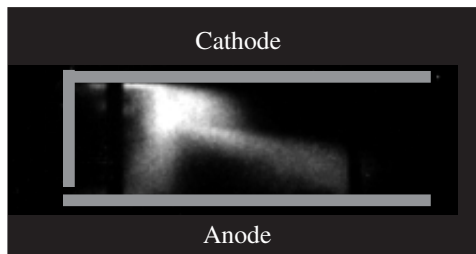


Figure 7: Imacon Fast Framing Picture of PT9 discharge (270  $\mu\text{F}$ , 4 J/pulse, 1  $\mu\text{g}$ /pulse) at 1.8  $\mu\text{s}$  after initiation with a 400 ns exposure. A narrow 488 nm line filter was used to pass only argon ion emission.

canting which could also eventually improve parallel-plate performance.

Parallel-plate geometries also allow the application of external magnetic fields that would augment the self-induced field and possibly increase performance as has been demonstrated in APPTs[8]. Due to the geometry of the electrodes and the use of only permanent magnets for the augmented fields, only a parallel-plate thruster can use this technique effectively. Future performance measurements at EP-PDyL will include the effects of applied magnetic fields in parallel-plate geometries.

## 6 Discussion and Conclusions

It has been shown through an analytic model of electromagnetic acceleration that two factors effect the performance directly: capacitance and inductance-per-unit-length. Although the performance scaling with the square-root of capacitance has been demonstrated experimentally, raising the capacitance to an arbitrarily high level is not beneficial as we have shown that the propellant utilization efficiency decreases at higher values of capacitance. Inductance-per-unit-length then becomes the next best parameter to maximize, however, performance data shows that this is not a simple task. In fact, although  $L'$  values are typically higher in parallel plate geometries, measured performance shows that co-axial electrodes with moderate values of  $L'$  have a higher efficiency and thrust-to-power ratio at the same operational conditions. Although inductance-per-unit-length does play a role in performance, it is only apparent as long as other loss mechanisms such as viscous wall losses associated with having these electrode configurations do not dominate the performance. In addition, there are other factors such as current sheet profile losses and discharge containment issues that suggest that co-axial electrodes are the best choice for an electromagnetic accelerator.

**Acknowledgments** The authors wish to thank John Blandino, Jay Polk, and Chris Salvo at NASA JPL for their support and the use of the Advanced Propulsion Group Facility.

## References

- [1] J.K. Ziemer, E.Y. Choueiri, and D. Bix. Is the gas-fed PPT an electromagnetic accelerator? an investigation using measured performance. In *35<sup>th</sup> Joint Propulsion Conference*, Los Angeles, California, June 20-24 1999. AIAA 99-2289.
- [2] J.K. Ziemer and E.Y. Choueiri. Performance and erosion measurements of gas-fed pulsed plasma thrusters at NASA jet propulsion laboratory. Technical Report EPPDyL-JPL99a, Princeton University, March 1999.
- [3] M.S. Di Capua. *Energy Deposition in Parallel-Plate Plasma Accelerators*. PhD thesis, Princeton University, 1971.
- [4] J.S. Cory. *Mass, Momentum and Energy Flow from an MPD Accelerator*. PhD thesis, Princeton University, 1971.
- [5] E. Antonsen, R.L. Burton, and F. Rysanek. Energy measurements in a co-axial electromagnetic pulsed plasma thruster. In *35<sup>th</sup> Joint Propulsion Conference*, Los Angeles, California, June 20-24 1999. AIAA 99-2292.
- [6] I. Kohlberg and W.O. Coburn. A solution for three dimensional rail gun current distribution and electromagnetic fields of a rail launcher. *IEEE Transactions on Magnetics*, 31(1):628–633, 1995.
- [7] T.E. Markusic and E.Y. Choueiri. Visualization of current sheet canting in a pulsed plasma accelerator. In *26<sup>th</sup> International Electric Propulsion Conference*, Kitakyushu, JAPAN, October 17-21 1999. IEPC 99-206.
- [8] H. Takegahara, T. Ohtsuka, and I. Kimura. Effect of applied magnetic fields on a solid-propellant pulsed plasma thruster. In *International Electric Propulsion Conference*, Tokyo, Japan, 1984. IEPC 84-50.

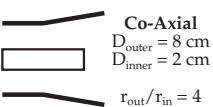
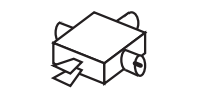
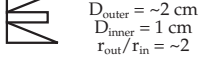

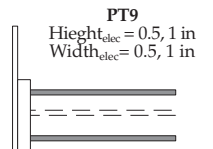
Thruster Name	Inductance Gradient (L')	Capacitance	Electrode Shape	Discharge Initiation (erosion rate)	Propellant Utilization
PT5 (8 kg)	280 nH/m	130 $\mu$ F 270 $\mu$ F	 <p><b>Co-Axial</b>  <math>D_{outer} = 8</math> cm  <math>D_{inner} = 2</math> cm  <math>r_{out}/r_{in} = 4</math></p>	4 Semi-Conductor Surface Flash-over Spark-plugs  (~0.2 $\mu$ g/shot)	Pulse Frequency: 3.7 kHz (Argon)  Electrode Length: 6.3 cm  $\eta_{pu} = 60\%$
Quad Thruster (PT6, PT7, PT8) (2.9 kg, 1.6 kg, 3.5 kg)	Co-Axial ~140 nH/m Parallel-Plate ~310 nH/m PT8 ~440 nH/m	63 $\mu$ F	 <p><b>Co-Axial</b>  <math>D_{outer} = 2</math> cm  <math>D_{inner} = 1</math> cm  <math>r_{out}/r_{in} = 2</math></p>  <p><b>Parallel-Plate</b>  Hieght<sub>elec</sub> = ~1 cm  Width<sub>elec</sub> = ~1 cm</p>  <p><b>PT8 (Ferrite)</b>  Hieght<sub>elec</sub> = ~1 cm  Width<sub>elec</sub> = ~2 cm</p>	<p><b>Co-Axial</b> 2 Semi-Conductor Surface Flash-over Spark-plugs</p> <p><b>Parallel-Plate</b> 1 Semi-Conductor Surface Flash-over Spark-plug (0.2 <math>\mu</math>g/shot)</p> <p><b>PT8</b> 1 RF Gas Breakdown Spark-plug (0.1 <math>\mu</math>g/shot)</p>	<p><b>PT6, PT7</b> Pulse Frequency: 3.7 kHz (Argon)  Electrode Length: 3.5 cm <math>\eta_{pu} = 33\%</math></p> <p><b>PT8</b> Pulse Frequency: 4.3 kHz (Argon) 5 kHz (H<sub>2</sub>O)  Electrode Length: 5 cm <math>\eta_{pu} = \sim 80\%</math></p>
PT9 (6 kg)	280 nH/m 390 nH/m 565 nH/m	130 $\mu$ F 270 $\mu$ F	<p><b>PT9</b> Hieght<sub>elec</sub> = 0.5, 1 in Width<sub>elec</sub> = 0.5, 1 in</p> 	2 0.01" Diameter Tungsten Trigger Wires  (unmeasured erosion rate)	Pulse Frequency: 4 kHz (Argon)  Electrode Length: 10 cm $\eta_{pu} = 100\%$

Figure 8: Table of the various GFPPTs tested and presented in this paper.